Oxygen Mass Transfer in Bubble Columns Working at Large Gas and Liquid Flow Rates

M. ALVAREZ-CUENCA,
and
M. A. NERENBERG

Engineering Science
The University of Western Ontario
London, Ontario, Canada N6A 5B9

One of the most persistent obstacles in the study of oxygen mass transfer in bubble columns is the technical difficulty of using large liquid and gas flow rates economically. This experimental limitation is reflected in the present, very incomplete, understanding of the mass transfer characteristics of these two-phase systems. In this work, a new experimental technique has been developed and used.

The use of computer-calculated concentration contour diagrams permitted a detailed study of the mass transfer characteristics of the zone near the distributor. No similar study has been reported in the literature until now. The ability of the axial dispersion and two-zone models to describe the experimental data is analyzed.

Finally, liquid side volumetric mass transfer coefficients have been calculated for both models. The results indicate that K_La increases, often linearly, with the superficial gas velocity. Furthermore, for the liquid-phase range [0, 10] cm/s, K_La had a minimum at $V_l \sim 7.5$ cm/s. For larger liquid superficial velocities, an increase in K_La was found. These observations were valid for the axial dispersion (*ADM*), plug flow (*PFM*) and two-zone (*T-ZM*) models.

SCOPE

Although no convention exists regarding their definition, bubble columns are reactors in which the gas phase rises, as bubbles, through a cocurrent or countercurrent flow of a continuous liquid phase. Thus, liquid or gas superficial velocities are neither limiting factors in this definition nor in their industrial applications (Ostergaard and Fosbol, 1972; Yoshida and Akita, 1965).

The industrial use of bubble columns is very widespread. They can be used as contactors, in which physical absorption or desorption takes place, and as chemical reactors. The large variety of applications, reviewed by Sharma and Mashelkar (1968), Mashelkar (1970), Deckwer (1977), and Alvarez-Cuenca (1979), illustrates the versatility of these devices. The use of bubble columns as fermentors is recent. However, a great deal of research on this application is taking place as shown by the work done by Todt et al. (1977), Hsu et al. (1977), Shioya et al. (1978), etc.

The experimental work published on concurrent bubble columns is not extensive enough to yield any reliable model or general correlation. The unification of the published studies on dispersion and mass transfer is very difficult, since those studies were invariably carried out under different experimental conditions. Even when similar flow conditions exist, it is not unusual to find two publications which not only differ in their results but also contradict each other. There are several reasons for this:

1) The lack of a valid mathematical model capable of describing the hydrodynamics of the system.

2) The existence of geometrical factors affecting the fluid flow (i.e., gas and liquid distributors, cross-section of the column, internals, etc).

3) The use of experimental methods that can affect the properties under study.

4) In most of the published literature, the gas and liquid superficial velocities are low, which adds to the aforementioned incompleteness.

The present investigation is concerned with mass transfer and dispersion in bubble columns. Specifically, values of the volumetric liquid-side mass transfer coefficient and axial dispersion coefficient in a bubble column are presented. Flow characteristics are analyzed with the help of contour diagrams. The *ADM* is shown to be inadequate to describe the present flow conditions. Finally, the *T-ZM*, developed in the present study, is compared with the *ADM*.

CONCLUSIONS AND SIGNIFICANCE

The use of contour diagrams has proven to be an attractive analytical tool in the study of bubble columns. This method can be extended to three-phase fluidized beds with spectacular results.

The presence of two well-differentiated mass transfer regions (namely, the grid zone and the bulk zone) confirmed the observations made with concentration profiles. Mass transfer near the grid was qualitatively and quantitatively different from that occurring in the bulk zone. In fact, 95% or more of the water oxygenation measured at the column exit can take place in the lower 20% of the column height (grid or distributor zone). In the bulk zone (the rest of the column height), the oxygen concentration was higher at the edges than along the central axis.

Pressure profiles in bubble columns are linear with distance except for $V_l = 2.5$ cm/s and $V_g = 28$ cm/s. Under these conditions, a large gas holdup appears in the upper portion of the column producing a small deviation from linearity.

The *ADM* gives no better description of the flow in bubble columns than the *PFM* does. The dispersion and mass transfer coefficients are very much a function of the sampling points

Correspondence concerning this paper should be addressed to M. Alvarez-Cuenca.
M. A. Nerenberg is with the Dept. of Applied Mathematics, The University of Western Ontario.

0001-1541-81-3367-0066-$2.00.

position at which they are calculated. This is a consequence of the different mass transfer mechanisms which exist in the grid and bulk zones. Thus, the *ADM* is too rigid a model to describe mass transfer and dispersion in these flow systems.

The two-zone model represents a significant improvement in the quantitative description of the mass transfer in bubble columns. The values of the mass transfer coefficient in the grid zone $(K_La)_{TG}$ were often several orders of magnitude larger than those of the mass transfer coefficient in the bulk zone $(K_La)_{TB}$.

The volumetric mass transfer coefficients increased, often linearly, with the gas superficial velocity. On the other hand, they decreased as V_l increased up to $V_l \sim 7.5$ cm/s. For larger values of the liquid superficial velocity, K_La increased. This was true independently of the model considered.

EXPERIMENTAL

The experimental system consists of four sections (Figure 1):
1) the column in which the experiments were made,
2) the air conditioning and regulatory system,
3) the water de-aeration system,
4) the sampling and analytical system.

The bubble column was 250 cm high, 66 cm wide, and 2.5 cm thick. It had more than 50 sampling points set along four lines (B, C, D, E) parallel to the main axis (Figure 2). These sampling points permitted a thorough mapping of the water oxygen concentration within the column. Pressure profiles along its main axis (Position C) were also measured.

The air-conditioning and supply system yielded oil-free air of a known humidity and flow rate. Gas superficial velocities were set at 4, 12, 20 and 28 cm/s. The air entered at the bottom of the column through four equally spaced nozzles.

The water, which followed a cyclic path, was initially collected in a 0.2 m^3 tank (M) which contained a stainless steel coil (N). Hot or cold water was passed through this coil to maintain the temperature of the liquid in the tank at 23.5 ± 0.5°C in all experiments. The water, which was pumped from the tank to the vacuum de-aerator (P) exited the latter to enter the bubble column (E) at superficial velocities of 2.5, 5, 7.5 and 10 cm/s. Finally, the water leaving the bubble column was again collected in the tank (M); thus, closing the cycle.

The sampling system consisted of an oxygen meter (H) and its probe (I), and the sampling cell connected to a graduated vessel which permitted to evaluate the sampling flow rate. The aforementioned system had two main objectives: 1) to produce samples representative of the conditions existing at a given point in the column and 2) to analyze those samples for dissolved oxygen.

The experimental system as well as the gas and liquid column distributors have already been amply described by Alvarez-Cuenca (1979) and Alvarez-Cuenca et al. (1980a).

RESULTS AND DISCUSSION

The results described herein have qualitative and quantitative aspects. Qualitative flow features which have a direct impact on mass transfer in bubble columns will be described, and a quantitative analysis of the mass transfer will be given. That analysis will be the basis for further considerations regarding the ability of the *ADM* and *T-ZM* to represent the flow in bubble columns.

FLOW PATTERNS IN BUBBLE COLUMNS

Concentration contour diagrams, concentration profiles, and pressure profiles constitute the base of the study of flow behavior in these two-phase systems.

The use of concentration contour diagrams in the study of flow patterns represented a very attractive complement to the

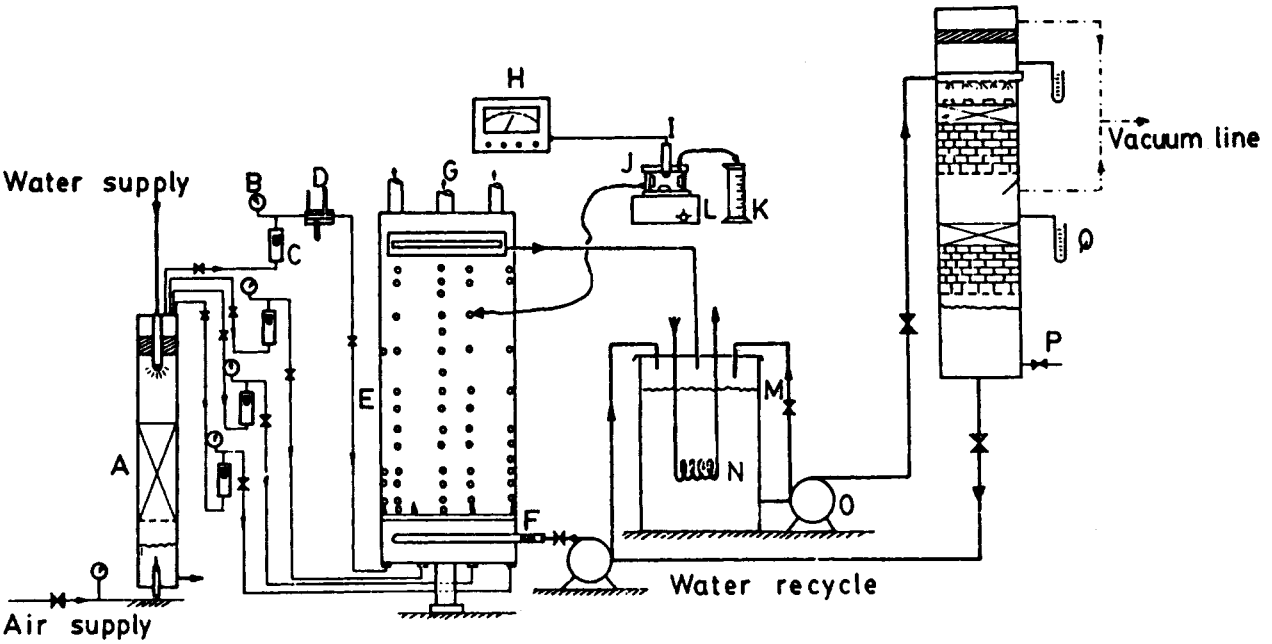

Figure 1. Schematic of experimental system.

A-Air Saturator	I-Oxygen Probe
B-Pressure Gauges	J-Mixing Cell
C-Air Rotameters	K-Vessel
D-Hygrometer	L-Magnetic Stirrer
E-Column	M-Tank
F-Venturimeter	N-Coil
G-Air Vents	O-Pumps
H-Oxygen Meter	P-Vacuum Deaerator
	Q-Manometers

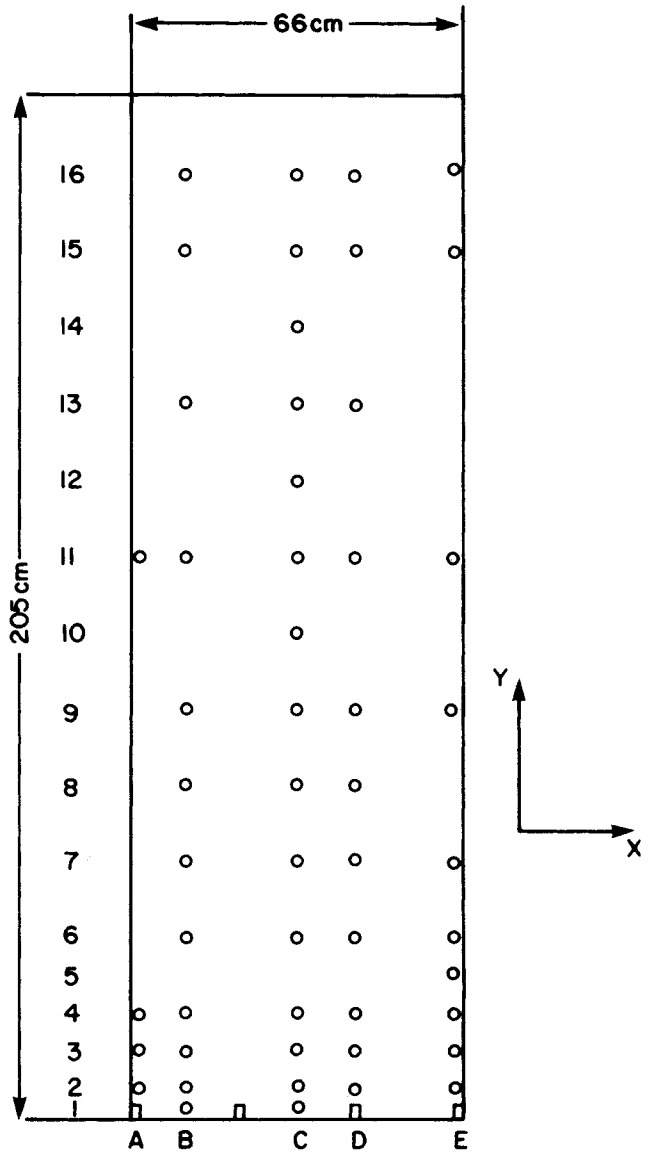

Figure 2. Sampling points distribution in the column.

pressure and concentration profiles. As described by Alvarez-Cuenca (1979) and Alvarez-Cuenca et al. (1980), contour diagrams are generated when a series of equally-spaced c = constant planes intercept a function of the form $c = \phi(x,y)$. This function, usually taken as a polynomial, results from fitting it to the experimental data obtained from mapping the column. A typical isogram (any line belonging to the diagram) is formed then by the loci of the points having the same concentration of oxygen in the liquid phase. Thus, a given set of discrete data can be employed to obtain a continuous static view of the oxygen concentration in the column. The spread, or lack thereof, of the isograms indicates the oxygenation gradient.

In Figures 3 and 4, the liquid phase has a long residence time (V_l = 2.5 cm/s), and this results in enhanced oxygenation. This is confirmed by the density of the isograms below y = 40 cm which indicates that most of the oxygenation measured at the column exit took place in the lower 20% of the column height which constitutes the grid zone. From the end of the grid region to the exit (bulk zone), only 0.3 mg/L of oxygen were transferred. The liquid phase oxygen concentration was ~ 3.5 mg/L at y = 2 cm and 6.4 mg/L at y < 40 cm.

The preponderant effects of the air jets in the grid region were even clearer in Figure 4. Again, the air jets sited at the grid produced concentrations in the range 6-6.5 mg/L at the grid (y = 2 cm), ~ 7.9 mg/L at the boundary of the grid and bulk zone and 8.2 mg/L at the exit of the column. Thus, only 0.3 mg/L was the

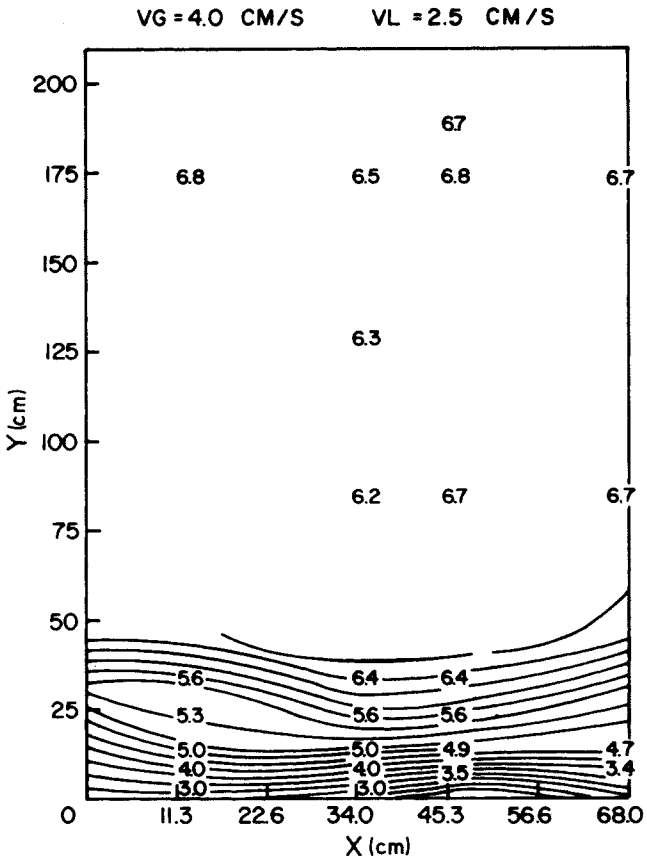

Figure 3. Oxygen concentration contour diagram (units: mg/L). The concentration gradient occurs in the first 50 cm of the column height. For y > 50 cm, the oxygen concentration remains virtually constant.

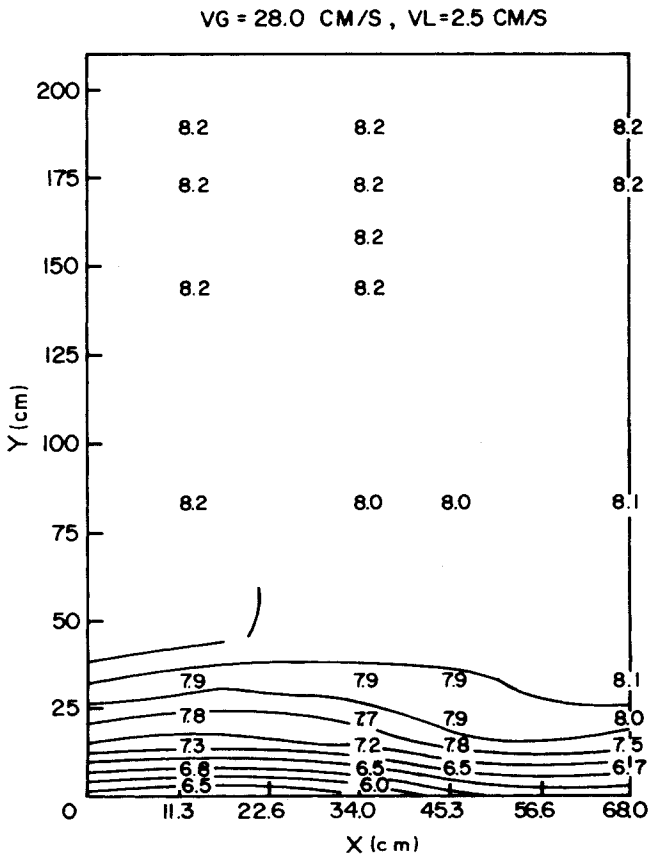

Figure 4. Oxygen concentration contour diagram (units: mg/L). Maximum gas velocity and liquid residence time favor rapid oxygenation near the grid or distributor.

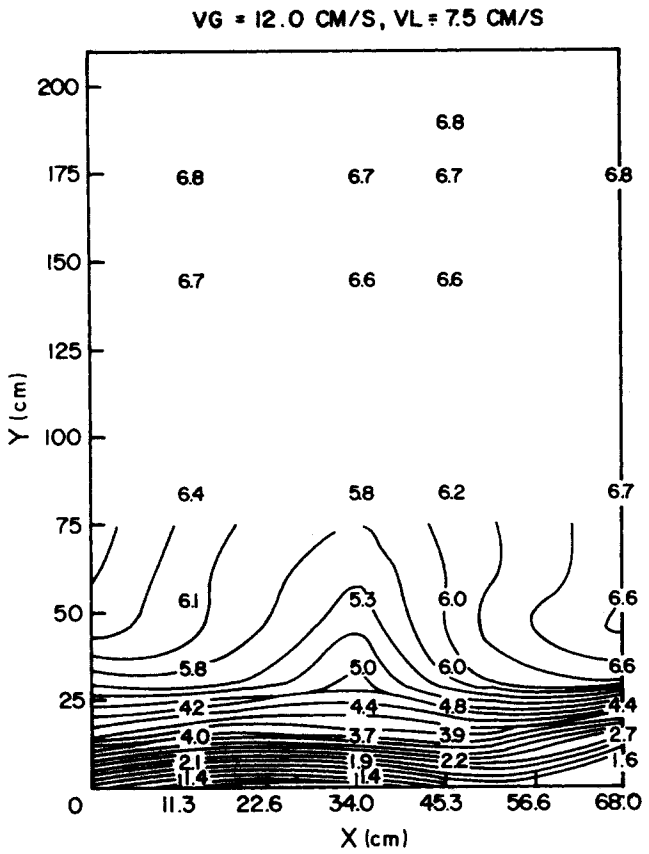

Figure 5. Oxygen concentration contour diagram (units: mg/L). Pseudoparabolic concentration profiles occurring in the column. At high liquid velocities and low gas velocities mixing is poor.

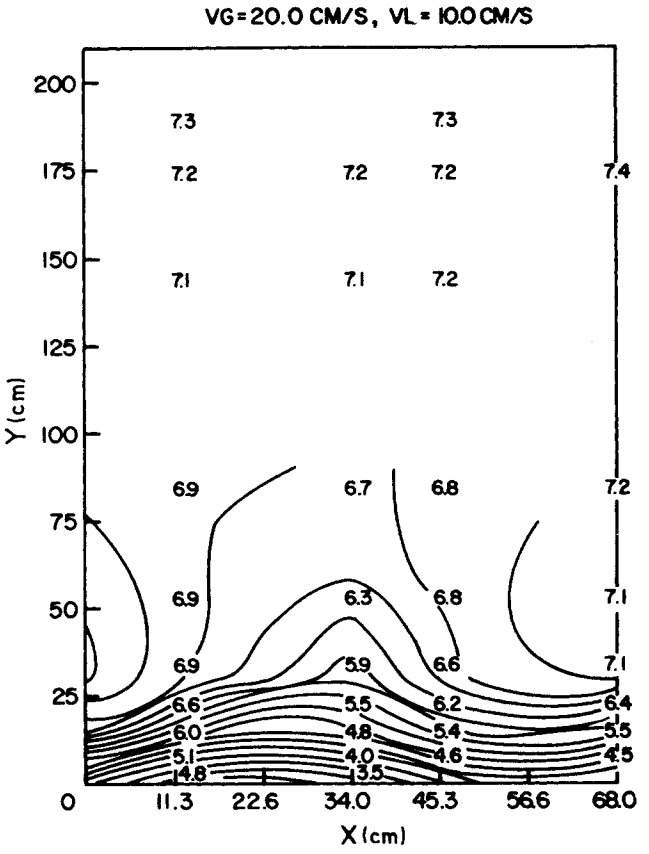

Figure 6. Oxygen concentration contour diagram (units: mg/L). The contour diagram is similar to the previous one. However, the increase in V_g and V_l produces a faster oxygenation in the column.

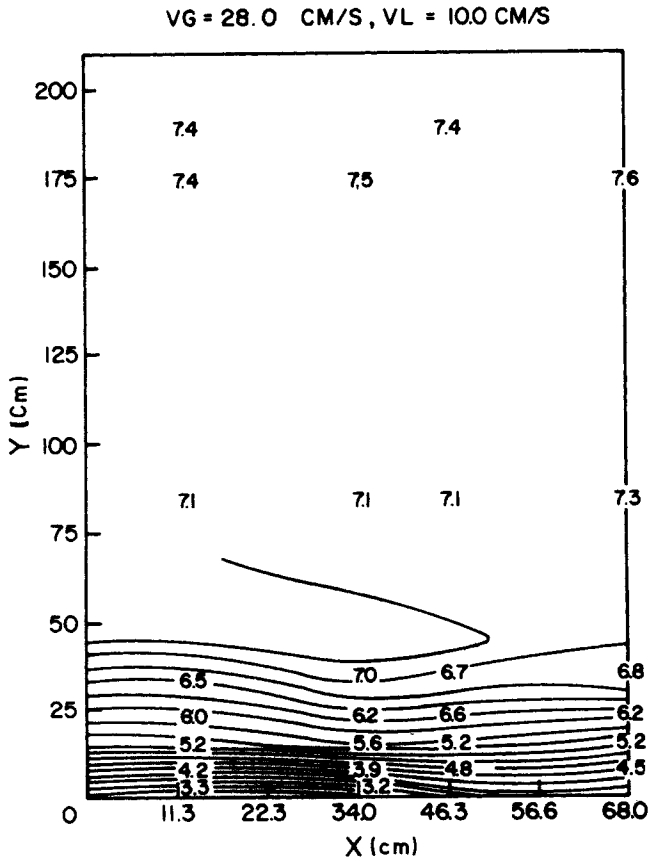

Figure 7. Oxygen concentration contour diagram (units: mg/L). Maximum gas and liquid velocities produce a good lateral mixing and high oxygenation near the grid.

contribution made by bubble mass transfer in the bulk zone.

The extent of the grid region decreased, as V_g increased from 4 to 28 cm/s. This is intuitively obvious, for as V_g increases so does the oxygenation rate, and saturation is reached at shorter distances from the distributor.

For V_l = 2.5 cm/s, the water has the longest residence time, thereby increasing oxygenation. The effect is more conspicuous for V_g = 28 cm/s. For intermediate values of V_g and large V_l (Figures 5 and 6), the isograms extend well past y = 50 cm reflecting a lower oxygenation rate. However, as shown in Figure 7, the rate increases again as V_l increases to 10 cm/s and V_g to 28 cm/s. This was explained by Alvarez-Cuenca et al. (1980), as the result of two competing mass transfer effects. At low V_l, the long liquid residence times favours oxygenation. When V_l is large, the residence time is short but the liquid enhances oxygenation near the distributor due to the breakdown of the air jets by the shear of the moving liquid.

A curious shape can be seen in Figures 5 and 6. When neither the gas velocity nor the liquid velocity is large enough to produce good lateral mixing as in the aforementioned diagrams, maxima are observed in the region of the central axis of the column. The maxima might be the consequence of pseudoparabolic velocity profiles. Therefore, along that axis V_l is larger and the oxygen concentration is lower. Indeed, these maxima in these two-dimensional representations correspond to depressions or valleys in a three-dimensional plot. Consequently, these maxima should, in reality, be visualized as regions of low oxygen concentration. At the edges of the column, a higher concentration of oxygen can be observed. This is evident since not only does the liquid have a lower velocity, but also "gulf stream" effects tend to increase the water residence time at these edges. The authors are not aware of contour diagrams having been used by others to analyze flow patterns in cocurrent gas-liquid systems. Therefore, no comparison with the findings of other workers is possible.

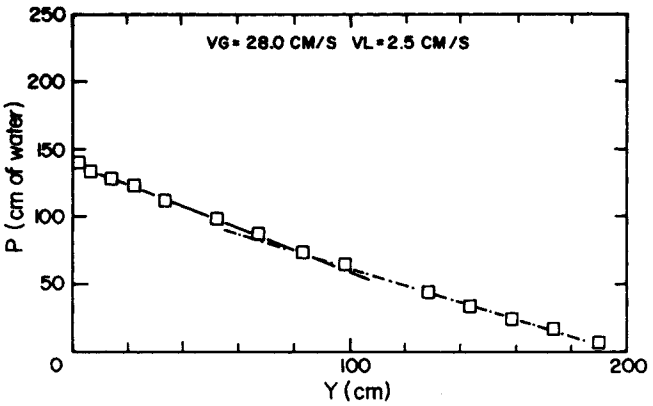

Figure 8. Pressure profile. Linearity is observed at the highest flow conditions.

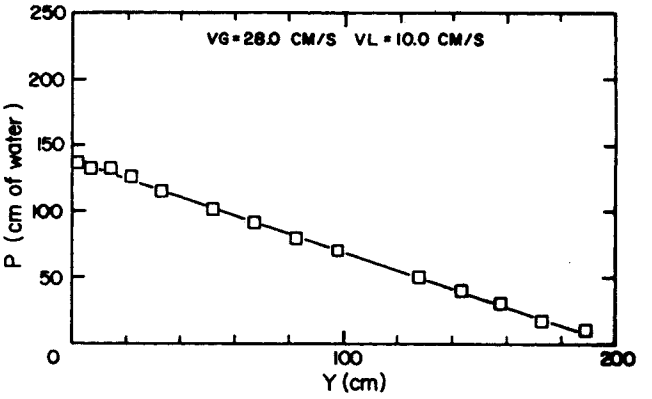

Figure 9. Pressure profile. A change in slope is observed at $y \simeq 100$ cm. Coalescence contributes to the reduction in the pressure gradient.

Pressure profiles were also used in the study of mass transfer characteristics of bubble columns (Figures 8 and 9). These profiles show that, except for $V_g = 28$ cm/s and $V_l = 2.5$ cm/s (Figures 9) in which the gas holdup is at a maximum, a linearly decreasing trend of pressure with the column height holds. Even at the aforementioned flow rates, deviations from linearity were small. The dotted line in Figure 9 corresponds to a region in which coalescence and gas holdup were high.

The flow features shown by the contour diagrams were complemented by the concentration profiles already presented elsewhere (Alvarez-Cuenca, 1979). The concentration profile, taken up the central axis of the column (Figure 10), served as the experimental data used to calculate the dispersion coefficients as well as the volumetric mass transfer coefficients.

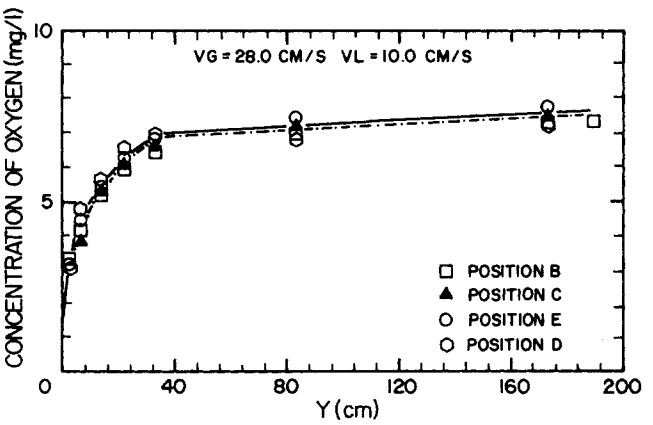

Figure 10. Concentration profiles at several positions in the column. The lateral mixing is perfect.

MODELS OF FLOW BEHAVIOR

The validity of a mathematical model is tested by its success in describing the experimental data. In this investigation, such a view has been adopted with respect to the *ADM* and the *T-ZM*. Furthermore, the necessity of having a flow model which can supply reliable mass transfer parameters is emphasized (this is specially necessary in the engineering design of bubble columns). These parameters are presented in the next section. From their analysis, one is able to judge the ability of the *ADM* and *T-ZM* to fit the present experimental data. The predicted concentration profiles, obtained through a computer optimization procedure, have been compared with the experimental data. For analyzing the fit of the aforementioned models to the data, two statistical parameters have been used as criteria. They are: the relative error (*RE*) between points of the predicted and data profiles, and the modified standard error of the fit (*MSE*). The *MSE* defined by Spiegel (1961) has properties similar to those of the standard deviation. Thus, a modified standard error of 0.3 mg/L indicates that 95% of the data pertaining to a concentration profile would lie within ±0.6 mg/L of the model fit line. More details have been given by Alvarez-Cuenca et al. (1980).

AXIAL DISPERSION MODEL

Alvarez-Cuenca (1979) and Alvarez-Cuenca et al. (1980) have shown that the *ADM* does not describe the flow in bubble columns better than the *PFM*. The fact is of interest given the large range of gas and liquid velocities used in their work. Deckwer (1979) and Deckwer et al. (1974) have claimed that ". . . the pertinent treatment of bubble column reactors should be based on the axial dispersion model." Nevertheless, their experiments were carried out at very low liquid velocities. Furthermore, they used porous plates as distributors. Those considerations differ drastically from the ones maintained in the present study.

The values of the axial dispersion coefficient (E_y) and mass transfer coefficient ($K_La)_D$ were obtained from the optimization of the analytical solution of the following: Eq. 1 subject to the boundary conditions Eqs. 2 and 3.

TABLE 1. MASS TRANSFER COEFFICIENTS $(K_La)_D$ FOR COMPLETE PROFILES

REGIME: BUBBLE COLUMNS

MODEL: AXIAL DISPERSION

V_g \ V_l	2.5	5	7.5	10
4	0.13	0.037	0.041	0.096
12	0.32	0.24	0.15	0.29
20	0.46	0.30	0.25	0.43
28	0.83	0.30	0.29	0.68

TABLE 2. MODIFIED STANDARD ERROR OF FIT TO EXPERIMENTAL DATA

REGIME: BUBBLE COLUMNS

MODEL: AXIAL DISPERSION

V_g \ V_l	2.5	5	7.5	10
4	2.5	1.6	1.0	1.8
12	2.0	1.7	1.6	2.0
20	1.9	1.8	1.8	2.0
28	1.5	1.9	1.6	1.7

TABLE 3. MODIFIED STANDARD ERROR OF FIT TO EXPERIMENTAL DATA

REGIME: BUBBLE COLUMNS

MODEL: TWO-ZONE

V_g \ V_l	2.5	5	7.5	10
4	0.79	0.32	0.21	0.28
12	0.97	0.58	0.39	0.83
20	1.2	0.66	0.34	0.89
28	1.2	0.81	0.76	0.78

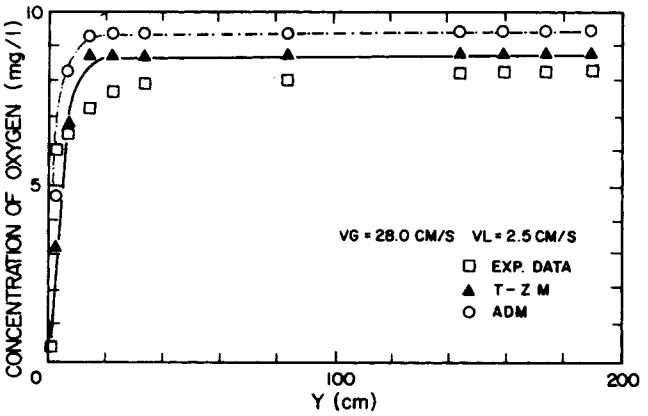

Figure 11. Experimental profile and those predicted by the models. The maximum gas velocity and minimum liquid superficial velocity produce the worst fits. Nevertheless, the *T-ZM* fits the data better than the *ADM*.

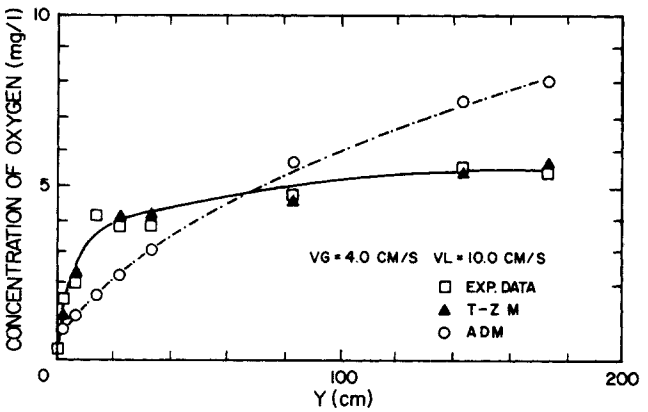

Figure 12. Excellence of the *T-ZM* fit to the data contrasts sharply with the fit of the *ADM*.

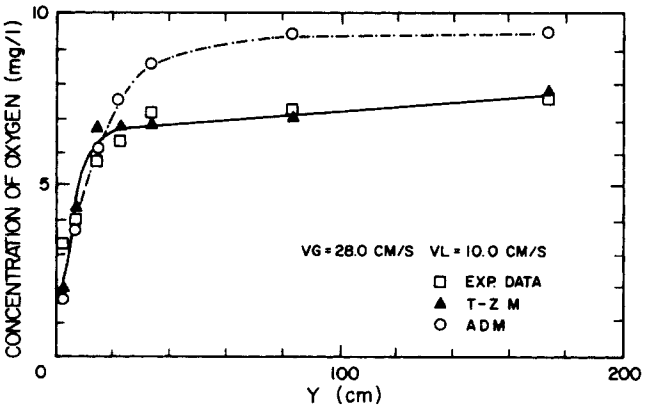

Figure 13. Under the highest flow rates, the *T-ZM* proves to give a far better fit than the *ADM*.

$$E_y \frac{d^2C}{dy^2} - V_l \frac{dC}{dy} + (K_La)_D (C^* - C) = 0 \quad (1)$$

$$V_l\, C(0^-) = V_l\, C\,(0^+) - E_y \frac{dC(0^+)}{dy} \quad (2)$$

$$\frac{dC(L^-)}{dy} = 0 \quad (3)$$

where $C(0^{\pm})$ is the concentration measured at a point immediately above (superscript +) or below (superscript −) the distributor, and L is the column length.

The solution of Eq. 1 has the form:

$$C = C^* + A\, e^{py} + B\, e^{ny} \quad (4)$$

where A, B, p and n are functions of E_y, V_l and $(K_La)_D$.

Values of the volumetric mass transfer coefficient are given in Table 1. However, their validity is very much negated by the large *MSE*'s shown in Table 2. Therein, it can be noticed that the modified standard error for all experiments is much larger than 0.6 mg/L. Thus, the *ADM* predicts very poorly the concentration profiles obtained under the present experimental conditions and its parameters, E_y and $(K_La)_D$, are meaningless.

The ability of the *ADM* to describe the mass transfer characteristics of bubble columns was further analyzed by optimizing the axial dispersion model in the bulk zone to fit the corresponding experimental data. The values of $(K_La)_D$ in the bulk zone were similar to those calculated by Deckwer et al. (1974) (the latter authors did not show concentration profiles in the grid region). This might be due to the use of porous plate distributors in conjunction with low gas and liquid superficial velocities. The values of the *MSE* in the bulk zone were lower than 0.3 mg/L in most of the cases. Thus, the fit in this region was excellent as opposed to that obtained for the entire column (Table 2).

The steep slope of the concentration profiles in the grid region made the dispersion coefficient tend to zero. In reality, E_y was found to be 0.1 cm²/s. Thus, the *ADM* evolved into the *PFM*. The type of boundary conditions used in solving the *ADM* for the complete profile had the same form as those for the bulk zone only. Notice that, as E_y tends to zero, the boundary condition at $y = 0$ becomes $C = C(0^-)$. Furthermore, the bulk zone alone was well represented by the *ADM*. It is concluded then that the boundary conditions were not responsible for the inability of the *ADM* to represent the flow in bubble columns. The origin of this inability lies in the existence of two well-differentiated regions in which the mass transfer mechanisms differ drastically.

Consequently, any model attempting to use the same parameters to describe mass transfer characteristics in both the grid and the bulk zones will be utterly inadequate, as the concentration profiles and contour diagrams show. In fact, no mathematical model which does not satisfactorily account for the mass transfer in the grid zone, where as much as 95% of the oxygenation occurs, can be considered adequate. An ampler view of this analysis is given by Alvarez-Cuenca (1979).

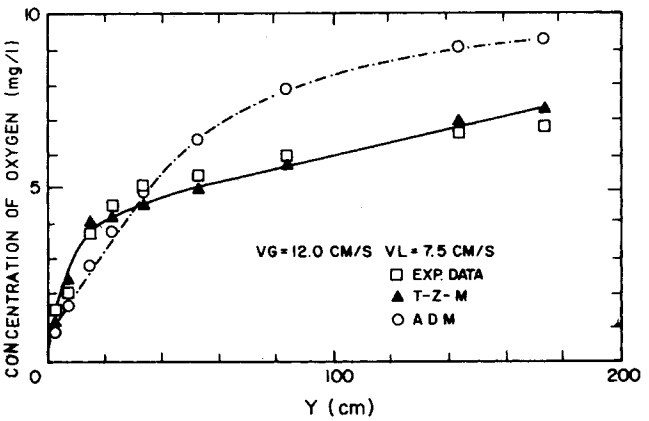

Figure 14. Fit of the *ADM* and *T-ZM* at intermediate flow conditions.

TABLE 4. MASS TRANSFER COEFFICIENTS IN GRID ZONE $(K_La)_{TG}$ *(in parenthesis)* AND BULK ZONE $(K_La)_{TB}$.

REGIME: BUBBLE COLUMNS

MODEL: TWO-ZONE

V_g \ V_l	2.5	5	7.5	10
4	(0.170) 1×10^{-3}	(0.161) 9×10^{-3}	(0.125) 1.7×10^{-2}	(0.325) 2×10^{-2}
12	(0.288) 2×10^{-5}	(0.430) 1.3×10^{-2}	(0.252) 4.2×10^{-2}	(0.477) 1×10^{-1}
20	(0.340) 2×10^{-5}	(0.375) 1.4×10^{-2}	(0.388) 3.4×10^{-2}	(0.682) 2.8×10^{-2}
28	(0.468) 2×10^{-5}	(0.396) 8.5×10^{-3}	(0.414) 5×10^{-2}	(0.825) 2.7×10^{-2}

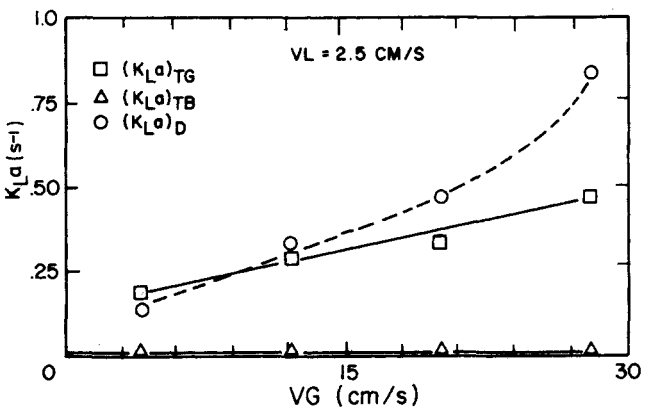

Figure 15. Volumetric mass transfer coefficients for the *ADM* and *T-ZM* against gas superficial velocity and V_l = 2.5 cm/s.

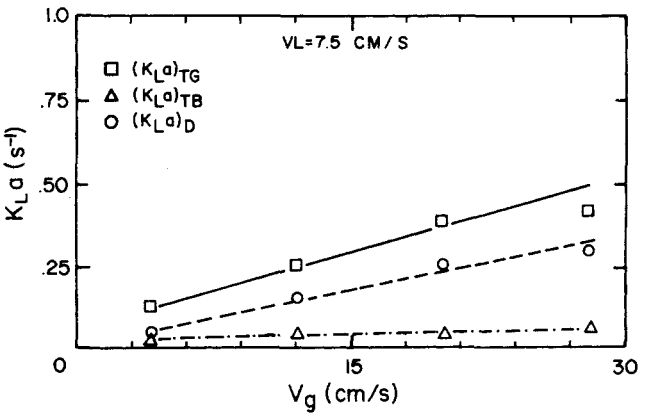

Figure 16. The same parameters as in Figure 15 are plotted at V_l = 7.5 cm/s.

TWO-ZONE MODEL

The *T-ZM* already described by Alvarez-Cuenca (1979) and Alvarez-Cuenca et al. (1980b) yielded the equations:

$$C = C^* - (C^* - Co)\, e^{-\alpha y} \tag{5}$$

in the grid zone $(0 < y < b)$ and

$$C = C^* - (C^* - C_o)\, e^{(\beta-\alpha)b}\, e^{-\beta y} \tag{6}$$

in the bulk zone $(y > b)$.

In these expressions $\alpha = (K_La)_{TG}/V_l$, $\beta = (K_la)_{TB}/V_l$, $(K_La)_{TG}$ and $(K_La)_{TB}$ are the volumetric mass transfer coefficients in the grid and bulk zone respectively and b is the height of the grid zone measured from the distributor.

As with the *ADM*, a summary of the values of the *MSE* for the two-zone model is presented in Table 3. A comparison between Tables 2 and 3 shows that the *MSE* is always much smaller for the *T-ZM* than for the *ADM*. Furthermore, as V_g/V_l increases, so does the *MSE*. This is confirmed by Figure 11. At V_g = 28 cm/s and V_l = 2.5 cm/s, the *T-ZM* has its worst fit, but was better than the axial dispersion model. At the lowest gas velocities (V_g = 4 cm/s), the fit is excellent (Figure 12).

For the maximum gas and liquid flow rates, namely V_g = 28 cm/s and V_l is 10 cm/s (Figure 13), the modified standard error is 0.78 and the fit is good despite the fact that the turbulence in the grid zone is at its highest. Figure 14 shows an interesting case in which the oxygen absorption takes place in a more uniform manner throughout the column as opposed to other profiles in which essentially no mass transfer occurs in the bulk zone (Figure 11). In both cases, the *T-ZM* is able to describe the data adequately.

As mentioned above, the two parameters describing the two-zone model are the mass transfer coefficients in the grid zone $(K_La)_{TG}$ and in the bulk zone $(K_La)_{TB}$. Table 4 illustrates their numerical difference as well as the trends observed by the coefficients with V_g and/or V_l. It can be seen that $(K_La)_{TG}$ passed through a minimum at middle values of V_l for a given velocity. This tendency, also observed by Alvarez-Cuenca (1979) in the *ADM* and *PFM*, can be explained as a result of two mutually counteracting effects. At low V_l, the long residence time of the liquid phase contributes to high mass transfer. As V_l increases, the residence time decreases and so does $(K_La)_{TG}$. However, as V_l increases an augmentation in the kinetic energy of the liquid phase contributes to the breakup of the air jets at the grid.

Thus, at a certain velocity in the range 5-7.5 cm/s, the turbulent effects which produce the increase in mass transfer balances the short residence time which tends to reduce the oxygenation. The increase in $(K_La)_{TG}$ with gas rate is particularly marked at constant V_l = 10 cm/s. In the bulk region, $(K_La)_{TB}$ also increases with both V_l and V_g. These trends confirm those found by Shulman and Molstad (1950), Houghton et al. (1957), Chen and Vallabh (1970), Hsu, et al. (1975, 1977). Investigators like Deckwer et al. (1974), Ostergaard and Suchozebrski (1968), and Ostergaard and Fosbol (1972) have observed K_La to be independent of V_l. Nevertheless, the gas and/or liquid velocities were low, and porous plate distributors were used. Under those conditions the jets are nonexistent. This means that the effect of the liquid velocity, particularly evident at the grid region in the present experiments, is minimal.

In a highly interesting paper, Deckwer et al. (1974) have claimed that the increase in the mass transfer coefficient in the grid region can be regarded as an end effect, which is constant for a given distributor configuration. The results of the present research contradict such a view since the oxygen concentrations (and mass transfer coefficients) at the grid were very much dependent on the gas and liquid flow rates. It is likely, however, that end effects play a more important role at low gas and liquid superficial velocities.

The effects of the superficial gas velocity on K_La are shown in Figures 15 and 16. The values of $(K_La)_D$ are intermediate between $(K_La)_{TG}$ and $(K_La)_{TB}$. The rate of increase in $(K_La)_{TB}$ with V_l is much smaller than that of $(K_La)_{TG}$.

ACKNOWLEDGMENT

The authors gratefully acknowledge research grants from the National Science and Engineering Research Council of Canada.

NOTATION

ADM = axial dispersion model
b = value of Y which marks the transition between the grid zone and bulk zone, cm
C = line of sampling points along the main axis of the column

C = concentration of dissolved oxygen in the liquid phase, mg/L
C^* = equilibrium concentration of dissolved oxygen, mg/L
C_o = concentration of dissolved oxygen at the grid ($Y = 0$); average measurement, ~0.5 mg/L
$CSTR$ = continuous stirred tank reactor
E_y = axial dispersion coefficient, cm^2/s
$(K_La)_D$ = volumetric mass transfer coefficient for the ADM, s^{-1}
$(K_La)_{TB}$ = volumetric mass transfer coefficient for the T-ZM (bulk zone), s^{-1}
MSE = modified standard error, mg/L
PFM = plug flow model
T-ZM = two-zone model
V_g = gas superficial velocity, cm/s
V_l = liquid superficial velocity, cm/s
x = x-axis in the concentration contour diagrams, cm
y = height of the sampling points measured from the grid (y=0), cm

Greek Letters

α = $(K_La)_{TG}/V_l$, cm^{-1}
β = $(K_La)_{TB}/V_l$, cm^{-1}
ϕ = two dimensional function obtained in the contour diagrams; relates the oxygen concentration at a point in the column to its position co-ordinates.

LITERATURE CITED

Alvarez-Cuenca, M., "Oxygen Mass Transfer in Bubble Columns and Three-Phase Fluidized Beds," Ph.D. Thesis, The University of Western Ontario, London, Ontario, Canada (1979).

Alvarez-Cuenca, M., M. A. Nerenberg, M. A. Bergougnou, and C. G. J. Baker, "Mass Transfer Models for Bubble Columns and Three-Phase Fluidized Beds," *29th Canadian Chem. Eng. Conference*, Sarnia, Ontario, Canada (1979a).

Alvarez-Cuenca, M., C. G. J. Baker, M. A. Nerenberg, and M. A. Bergougnou, "Oxygen Mass Transfer in Bubble Columns Working at Large Gas and Liquid Flow Rates," *Symp. on Fundamental Research in Heat and Mass Transfer*, Annual AIChE Meeting, San Francisco, CA (1979b).

Alvarez-Cuenca, M., M. A. Bergougnou, and M. A. Nerenberg, "Oxygen Mass Transfer in Three-Phase Fluidized Beds Working at Large Flow Rates," *International Conference on Fluidization*, Henniker, New Hampshire (1980).

Alvarez-Cuenca, M., C. G. J. Baker, and M. A. Bergougnou, "Oxygen Mass Transfer in Bubble Columns," *Chem. Eng. Sci.*, **35**, 1121 (1980a).

Alvarez-Cuenca, M., M. A. Nerenberg., and M. Bergougnou, "Oxygen Transfer in Bubble Columns and Three-Phase Fluidized Beds," *VI International Fermentation Symposium*, Paper No. F7.1.12P, London, Ontario (1980b).

Chen, G. H. and R. Vallabh, "Hold-Up and Mass Transfer in Bubble Columns Containing Screen Cylinders," *Ind. Eng. Chem. Proc. Des. Devel.*, **9**, 121 (1970).

Deckwer, W-D., R. Burckhart, and G. Zoll, "Mixing and Mass Transfer in Tall Bubble Columns," *Chem. Eng. Sci.*, **29**, 2177 (1974).

Deckwer, W-D., I. Adler, and A. Zaidi, "A Comprehensive Study on CO_2—Interphase Mass Transfer in Vertical Cocurrent and Countercurrent Gas-Liquid Flow," *Can. J. of Chem. Eng.*, **56**, 43 (1978).

Deckwer, W-D., "Bubble Column Reactors—their modelling and dimensioning," *Int. Chem. Eng.*, **19** (1), 21 (1979).

Houghton, G., A. M. McLean, and P. D. Ritchie, "Absorption of Carbon Dioxide in Water Under Pressure Using a Gas-Bubble Column," *Chem. Eng. Sci.*, **7**, 26 (1957).

Hsu, K. H., L. E. Erickson, and L. T. Fan, "Pressure Drop, Gas Hold-Up, and Oxygen Transfer in Tower Systems," *Biotech. and Bioeng.*, **19**, 247 (1977).

Hsu, H. H., K. B. Wang, and L. T. Fan, "Oxygen Transfer and Absorption Efficiencies in Bubble Columns," *Water and Sewage Works* (1975).

Mashelkar, R. A., "Bubble Columns," *British Chem. Eng.*, **5** (10), 1297 (1970).

Ostergaard, K., and W. Suchozebrski, "Gas-Liquid Mass Transfer in Gas-Liquid Fluidized Beds," *Proc. 4th European Symposium Chem. Reactor Eng.*, Pergamon Press, Oxford 21 (1968).

Ostergaard, L. and P. Fosbol, "Transfer of Oxygen Across the Gas-Liquid Interface and Gas-Liquid Fluidized Beds," *Chem. Eng. J.*, **3**, 105 (1972).

Shioya, S., N. D. P. Dang, and I. Dunn, "Bubble Column Fermenter Modelling: A comparison for pressure effects," *Chem. Eng. Sci.*, **33**, 1025 (1978).

Sharma, M. M. and R. A. Mashelkar, "Absorption with Reaction in Bubble Columns," *Inst. Chem. Eng. Symp. Series*, **28**, 10 (1968).

Spiegel, R. M., *Statistics*, McGraw Hill Inc., New York (1961).

Todt, J., J. Lucke, L. Schurgel, and A. Renken, "Gas Hold-Up and Longitudinal Dispersion in Different Types of Multiphase Reactors and Their Possible Application for Microbial Processes," *Chem. Eng. Science*, **32**, 369 (1977).

Yoshida, F. and K. Akita, "Performance of Gas Bubble Columns: Volumetric Liquid-Phase Mass Transfer Coefficient and Gas Hold-Up," *AIChE J.*, **11**, 9 (1965).

Manuscript received March 3, 1980; revision received July 14, and accepted July 16, 1980.

Bacterial Population Dynamics in Batch and Continuous-Flow Microbial Reactors

Calculations of the distribution of states in cell populations grown in well-mixed, isothermal batch and continuous flow reactors are presented. By restricting the analysis to a class of bacteria for which cell division control may be modeled using overlapping timers, analytical results are obtained for many cell population characteristics in terms of the growth rate history. This required growth rate trajectory is evaluated using a separate overall reactor model. The simulation results conform qualitatively to available experimental data and suggest new experiments for further testing of the single-cell model.

Y. NISHIMURA
and
J. E. BAILEY
Department of Chemical Engineering
University of Houston
Houston, TX 77004

SCOPE

Many processes, including reactors used to grow microorganisms or to utilize their catalytic assemblies, involve dispersed phases or entities. It has long been recognized that the performance of such processes depends in general on the distribution of states over the individual particles which constitute the dispersed phase. Process mathematical modeling which includes determination of the distribution of states usually leads to population balance equations (Fredrickson et al., 1967; Ramkrishna, 1979). These models, typically of integro-partial differential equation form, are rarely amenable to analytical

Y. Nishimura is on leave from Nagoya University, Nagoya, Japan.
Correspondence concerning this paper should be addressed to his current address: Department of Chemical Engineering, California Institute of Technology, Pasadena, CA 91125.